

Electrochemical Activation of Aluminum by the Addition of Tin, in 3% NaCl

Youssef Gouale,^{*} Salma Khatbi and Mohamed Essahli

*Laboratory of Applied Chemistry and Environment,
Faculty of Science and Technology, Univ. Hassan I, P.O. Box 5777, Settat, Morocco*

Received January 14, 2017; accepted September 15, 2018

Abstract

The aim of our studies was to show the effect of the addition of tin to aluminum in a solution of sodium chloride (NaCl 3%), by weight, as well as the influence of the alloy immersion time on its corrosion resistance. To do this, we have used, as electrochemical techniques, potentiodynamic polarization and electrochemical impedance spectroscopy and, as metallurgical techniques, hardness parameters and optical microscopy performed on the alloys made of pure aluminum (99.99%) and pure tin (99.99%). The obtained results show that the addition of tin enhances aluminum electrochemical activation, as well as the spontaneous formation of an oxide layer containing Al₂O₃, which then protects the metal from further corrosion. During all that process, the alloy immersion in 3% NaCl acts by promoting tin's attack and the alloy's corrosion.

Keywords: corrosion, activation, aluminum, tin, NaCl, alloy.

Introduction

Aluminum alloys are used in many sectors, such as automobile and aerospace industries and, very recently, in the field of energy storage batteries, as well as in various aggressive environments, due to its excellent resistance to corrosion [1].

The polarization of high-purity aluminum, in the cathodic sense, in neutral electrolytes, is characterized by the increase in the hydrogen evolution rate beyond a certain limit of the negative potential, as well as by the increase in the metal's dissolution rate. In this case, a number of phenomena could be expected to appear, including hybride's training [2-4].

Aluminum alloys' high corrosion resistance is due to the capacity of their surface to become very passive; this is linked to a quick aluminum reaction with oxygen, which allows creating a thin and amorphous oxide layer [5-8].

Thanks to this oxide layer formed onto the surface, the aluminum alloys are more resistant to corrosion. However, in corrosive environments, aluminum alloys, in contact with the atmosphere, are subject to pitting corrosion, stress corrosion cracking, corrosion fatigue and general attack corrosion. Aluminum is very

^{*} Corresponding author. E-mail address: gouale.youssef@gmail.com

resistant to rural atmospheres and marine areas and, conveniently, to the industrial atmosphere, depending on the pollutants proportions. Aluminum is protected by zinc and magnesium, but it is corroded by lead and tin. In these last cases, there must be provision for specific protections to avoid the phenomenon of galvanic corrosion. [9-15]

The objective of our work was to develop alloys based on aluminum, which can very well be used as anodes with a better electrochemical activation, for the cathodic protection of materials, while having a better hardness and resistance to mechanical shock.

Experimental procedure

Elaboration of alloys

The alloys were melted at 70 °C in a crucible. The choice of a good melting crucible is not always simple, given the wide range of materials, forms and capabilities. When it comes to choosing a crucible that will allow a good homogeneity of our elements, and that will have a good resistance to high temperatures, it is important to consider how and for how long it will be used. For our study, we have chosen one with 4 cm in diameter. After fusion and cooling until the total solidification was achieved, the ensemble (alloy-crucible) was soaked in water.

We used an electrode made of an Al-Sn alloy, with different contents of tin (2%, 4% and 6%), in the form of a disk of 1 cm². In order to obtain reliable and reproducible results, the working electrode underwent, before each test, polishing with different abrasive papers of 400, 600 and 1200 grit size. Then, it was rinsed with distilled water and dried.

The alloys were prepared from metals of 99.5% purity. The contents of Sn and the melting temperature were chosen in accordance with the phase diagram of the binary Al-Sn system represented in Fig. 1. The binary system of Al-Sn presented an eutectic bearing at 228.3 °C. The composition of the eutectic liquid was approximately 0.5% by weight of tin.

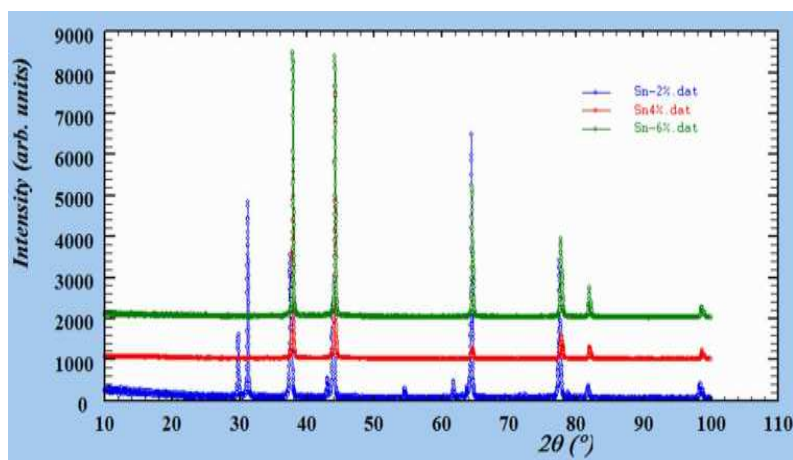


Figure 1. Phase diagram of the binary Al-Sn system.

Before elaborating the Al-Sn alloys, we have analyzed the chemical composition

of pure Al. After the elaboration of the alloys, we also have analyzed them, to know the exact chemical composition of each element, including the impurities. For this, we have used the “The Thermo Scientific Niton XL5”, which is a spectrometer of X-ray fluorescence. It is the newest and faster analyzer in the market nowadays, and it gives fast and accurate results. The chemical composition of the prepared alloys is represented in Table 1. It is a punctual analysis; therefore, the measurements were made at one point of each alloy.

Table 1. Chemical composition of Al and Al-Sn alloys.

Added Sn (%)	Al (%)	Sn (%)	Cr (%)	P (%)	Ti (%)	Si (%)	Cu (%)	Pb (%)	Mn (%)	Mg (%)	Zn (%)
0	99.50	-----	0.05	-----	-----	0.28	0.05	-----	0.03	0.02	0.07
2	97.91	2.00	0.001	0.01	-----	0.07	0.00	-----	-----	-----	-----
4	95.92	4.01	-----	-----	0.02	-----	-----	0.01	-----	0.02	-----
6	93.86	6.00	0.014	0.03	0.00	0.00	-----	-----	0.07	-----	0.01

Preparation of the NaCl solution

The solutions were prepared by dissolution of NaCl in distilled water. The test solutions were freshly prepared before each experiment. For each analysis, the experiment was made thrice to ensure the reproducibility of the results.

X-ray diffraction

The X-ray spectra of the three samples was obtained at room temperature, using a D2 PHASER Bragg-Brentano geometry diffractometer, with Cu Ka = 1.5406 Å (40 kV, 40 mA) type of radiation, and the 2θ scanning range was from 15 to 100 °, with a step of 0.01 (2θ).

Hardness

The hardness tests were carried out by the Vickers method, using a Testwell durometer under a load of 2 Kg. Each measurement corresponds to the average of a maximum of four imprints located on a planar section equivalent to a diameter plan, or perpendicular to the axis of the cylindrical sample. The sections were obtained by sawing, mechanical abrasion and then chemical polishing. Recall that the empirical relationship $HV = 0.3 R$ (MPa) can be used to assess the maximum load (R) of these alloys.

Optical microscopy

The physical properties of the quenched solid solutions of aluminum alloys evolved at room temperature. The hardening mechanisms were continuous/discontinuous transformations. This temperature corresponds to 0.5 TF (melting temperature of the alloy). We know that from 0.4 up to 0.5 TF, the elements of the alloy can diffuse. In the case where the kinetics of the discontinuous transformation was rapid at room temperature, we have used the original technique developed by Hilger [16].

Electrochemical techniques

The electrochemical measurements have been carried out in a cell of 3 electrodes consisting of a saturated calomel reference electrode, a platinum auxiliary

electrode and an Al-Sn working electrode. Before each test, the alloy was left under an open current for 5 min to achieve a stable state. For this study, we have used 2 types of electrochemical techniques: potentiodynamic polarization and electrochemical impedance spectroscopy (EIS). The potentiodynamic polarization was made by sweeping the potential at a speed of 5 mV/s, from -1500 to 0 mV. We have obtained different kinetic parameters such as corrosion current density (I_{corr}), corrosion potential (E_{corr}) and Tafel slopes (anodic β_a) and cathodic (β_c). The corrosion current density has been measured by extrapolation of Tafel straight lines. The measurements of the electrochemical impedance spectroscopy were performed using a margin of frequency ranging from 30 MHz to 50 kHz at the corrosion potential. For the analysis, we have used a 10 VoltaLab model (PGZ100) device connected to a HP computer with VoltaMaster 4 and OriginLab software for the data acquisition.

Results and discussion

X-ray diffraction

The X-ray diffraction shows that precipitates are of Al type (represented in Fig. 2). Furthermore, Sn element did not participate to the mechanisms of structural hardening of Al-Sn alloys. The influence of tin was reflected by an increase in hardness.

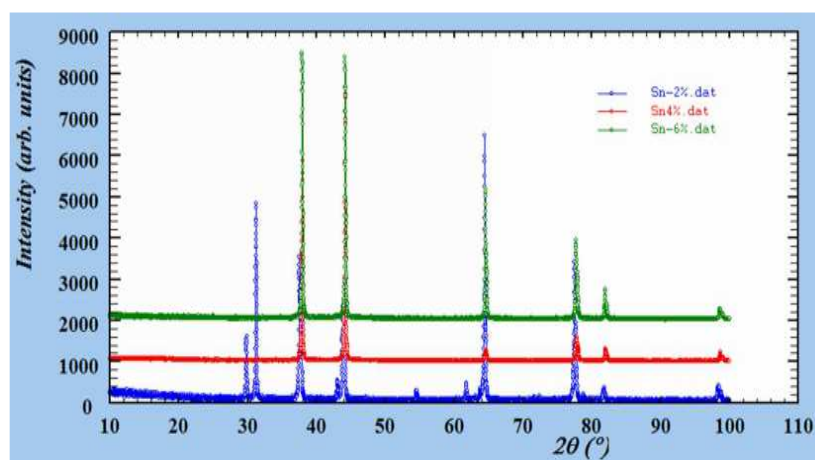


Figure 2. X-ray diffraction spectra of the cast alloys: Al-2%Sn, Al-4%Sn and Al-6%Sn, at 20 °C.

Hardness

Fig. 3 shows the hardness evolution in function of time. At 20 °C, the Al-2%Sn oversaturated hardened cast alloy had a hardness of 11.15 HV, which is almost the double of that of pure aluminum. This shows that the alloy was already partially transformed during cooling. At room temperature, the maximum hardness was reached at the end of one day (11.45 HV), and then the hardness slightly decreased and stabilized, to achieve 11.29 HV at the end of 5 days. For the Al-6%Sn alloy, the figure shows an increase in the hardness as a function of time, compared to the first sample gross casting, at room temperature. At room temperature, the maximum hardness was reached at the end of one day (11.55

HV); then, it slightly decreased, to achieve 11.25 HV after 5 days. According to the obtained hardness curves, it was shown that the alloys with the highest content of Sn (4% and 6%) were harder than with the content of Al-2%Sn (the addition of tin actually increases aluminum hardness, so, it becomes more resistant to mechanical shocks). These curves show that, as tin concentration increased, the aging process seemed to be more delayed. Also, the highest tin content (6%) resulted in a slight increase in the hardness, which was probably due to the solid solution of Al-Sn.

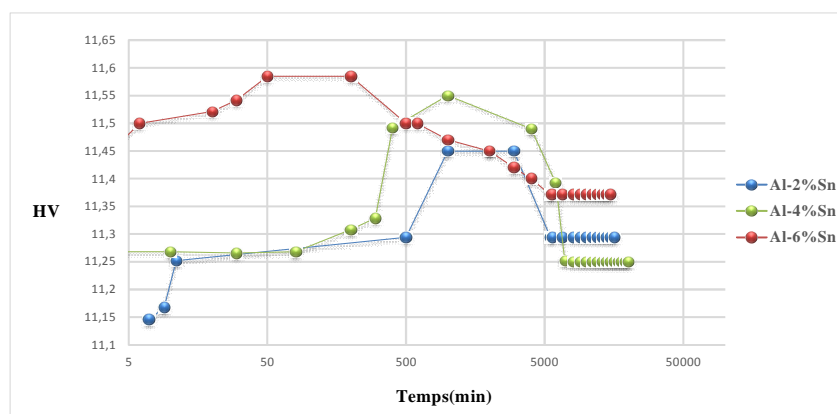


Figure 3. Hardness evolution as a function of time, at room temperature, of Al-Sn cast alloys immersed in water.

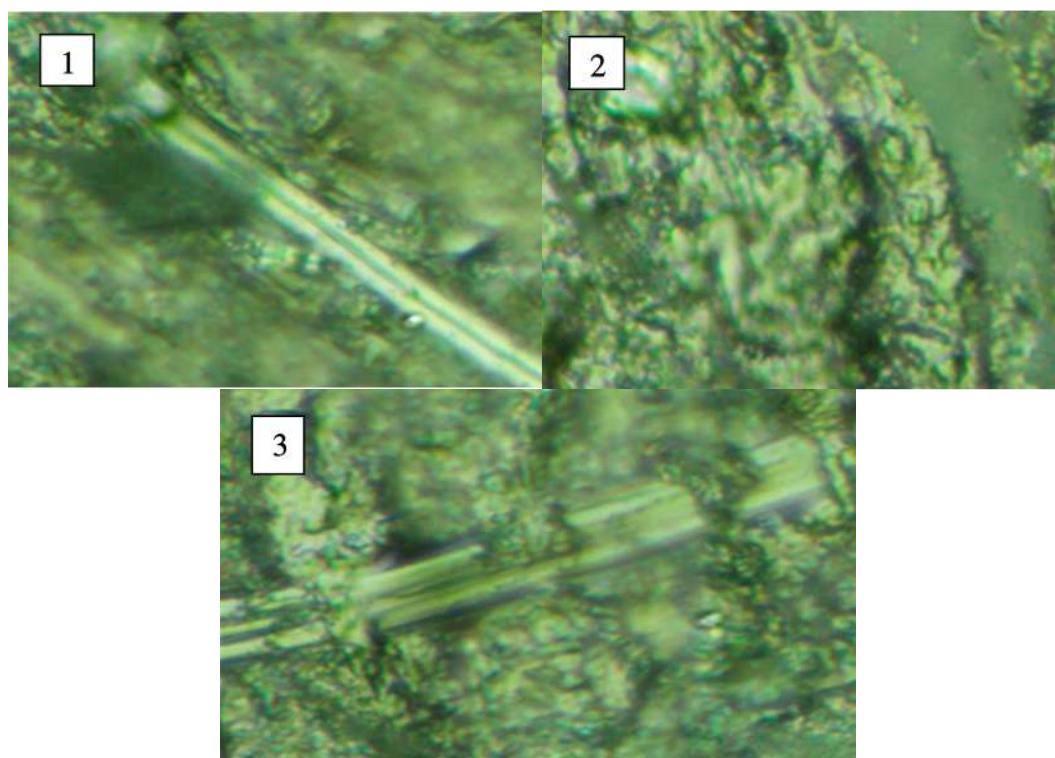


Figure 4. Discontinuous precipitation Al-2%Sn (1), Al-4%Sn (2) and Al-6%Sn (3) at 20 °C, after 20 days of aging.

Optical microscopy

Fig. 4 shows the visualization by optical microscopy of the precipitates aligned in

the discontinuous precipitation characterizing over aging. The analysis carried out in the regions affected by over aging shows that the precipitates are fully trained of Sn. However, the analyses of the interlamellar areas are much depleted of tin, and its concentration remains the same throughout the matrix.

Electrochemical techniques

Electrochemical impedance spectroscopy

The Nyquist plots shown in Fig. 5 are in the form of a single half-circle; this indicates that the charge transfer was the principal reaction mechanism at the interface of Al-Sn alloys.

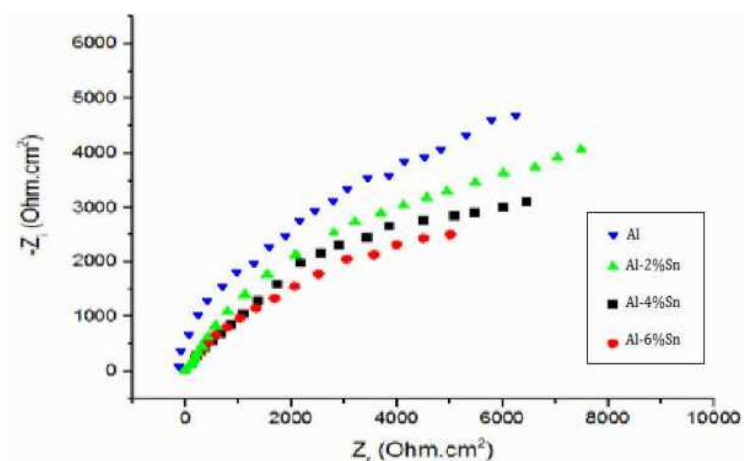


Figure 5. Nyquist plots of Al-Sn alloys with different concentrations of tin in 3% NaCl.

Table 2. Dielectric parameters characterizing the impedance diagrams of the effect of Sn addition on the corrosion of Al in 3% NaCl, at 25 °C.

Alloy	R _t (ohm.cm ²)	C _{dl} (μF/cm ²)
Pure Al	35.52	19.76
Al-2%Sn	32.24	24.68
Al-4%Sn	28.81	63.11
Al-6%Sn	11.45	104.93

The parameters represented in Table 2 show that the increase in Sn content led to a decrease in R_t (32.24 ohm.cm² for Al-2%Sn to 11.45 ohm.cm² for Al-6%Sn) and an increase in C_{dl} (24.68 μF/cm² for Al-2%Sn to 104.93 μF/cm² for Al-6%Sn). This means that the resistance of the layer that covers aluminum is higher than in the case of pure aluminum, which is more fragile, and the capacity of the double layer of the metal increases with the increase in Sn content.

It can be easily noted that, with the increase in the tin content, the diameter of the half-circles decreased, meaning that the addition of Sn led to the Al electrochemical activation. This indicates that the Al₂O₃ oxide layer, which was spontaneously formed onto the aluminum surface in contact with air, degraded after Sn addition. Tin infiltrates into the layer of Al₂O₃ and modifies its crystalline structure, leading to its degradation and to aluminum reactivation, which makes Al electro-chemically active and able to be used as an anode for cathodic protection systems.

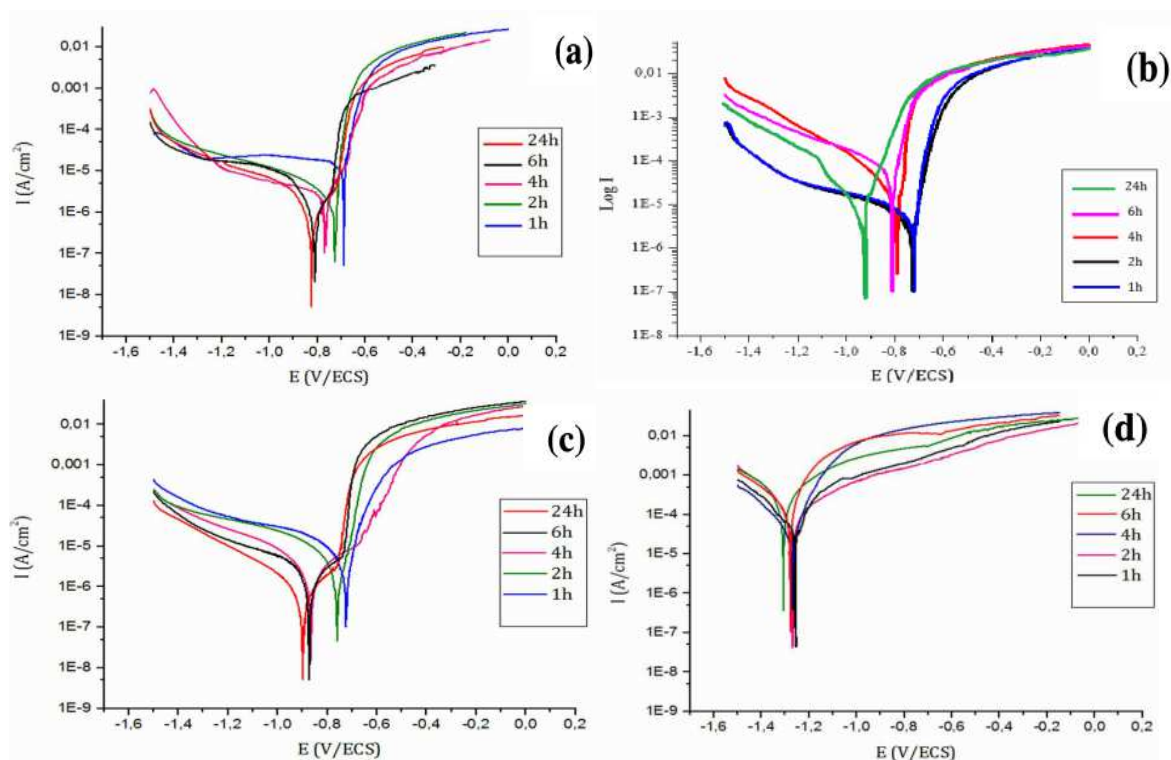


Figure 6. Polarization curves of immersion time effect on pure Al (a), Al-2%Sn (b), Al-4%Sn (c) and Al-6%Sn (d), in 3% NaCl.

Table 3. Polarization I-E curves parameters of pure Al and of Al-2%Sn, Al-4%Sn and Al-6%Sn alloys in 3% NaCl.

Alloy	Immersion time	E_{corr} (mV/ECS)	I_{corr} ($\mu\text{A}/\text{cm}^2$)	R_p ($\mu\text{A}/\text{cm}^2$)	β_a	β_c
Pure Al	1h	-701	0.61	7.8.10	-109	94
	2h	-728	0.80	5.4.10	-115	78
	4h	-758	1.04	3.2.10	-102	55
	6h	-768	1.45	2.9.10	-104	32
	24h	-812	1.70	2.1.10	-107	99
Al-2%Sn	1h	-710	1.87	5.2.10	-120	41
	2h	-723	2.03	6.0.10	-103	39
	4h	-793	2.79	4.7.10	-110	52
	6h	-801	3.51	3.1.10	-98	48
	24h	-854	8.53	2.5.10	102	60
Al-4%Sn	1h	-711	2.11	5.4.10	-135	33
	2h	-770	3.08	8.3.10	-108	40
	4h	-877	3.12	4.5.10	-101	49
	6h	-875	7.55	2.1.10	-99	66
	24h	-901	9.22	1.2.10	-108	76
Al-6%Sn	1h	-1225	13.08	7.26.10	-160	70
	2h	-1280	22.67	5.33.10	-120	35
	4h	-1272	45.44	4.22.10	-132	40
	6h	-1272	98.12	3.12.10	-117	44
	24h	-1310	127.20	1.16.10	-122	88

Potentiodynamic polarization

Influence of immersion time

The anodic and cathodic polarization diagrams of the Al-Sn alloys (with different contents of Sn) in 3% NaCl are represented in Fig. 6.

The intersection point of the Tafel lines gives the corrosion current density (I_{corr}). The obtained polarization parameters (I_{corr} , E_{corr} , β_a and β_c) are represented in Table 3.

After analyzing the polarization curves represented in Fig. 6, as well as the polarization parameters in Table 3, we can clearly see that the immersion time acts in a similar way for all the alloys; the more the electrode is immersed in 3% NaCl, the more the corrosion potential (E_{corr}) is shifted to the anodic potentials (from -701 mV/ECS to -812 mV/ECS, for Al-2%Sn, as example) and the more the corrosion current density (I_{corr}) increases (up to 127.20 $\mu\text{A}/\text{cm}^2$ for Al-6%Sn), meaning that the immersion time acts on the alloys by increasing their corrosion. Also, the addition of tin moves the corrosion potential towards more electronegative potentials (from -701 mV/ECS for pure Al up to -1225 mV/ECS for Al-6%Sn). Additionally, it increases the corrosion current density (from 0.61 $\mu\text{A}/\text{cm}^2$ for pure Al up to 13.08 $\mu\text{A}/\text{cm}^2$ for Al-6%Sn), indicating that the addition of tin leads to electrochemically active aluminum. These results are in very good agreement with those of the electrochemical impedance spectroscopy.

Conclusions

In this work we have tested different alloys based on aluminum (Al-2%Sn, Al-4%Sn and Al-6%Sn) in a solution of 3% NaCl, so that they could be used as anodes for cathodic protection. The confrontation of experimental results was obtained with the used electrochemical methods, namely, potentiodynamic polarization and electrochemical impedance spectroscopy, which have allowed us to identify the main phenomena governing the reaction mechanism at the electrode/electrolyte interface.

The studies made on the Al-Sn alloys show that the addition of Sn to aluminum has led to more active alloys. This activity is indicated by a shift of the corrosion potential towards more negative values, and also to a reduced passivity of aluminum.

The immersion time of the alloys and the addition of tin favors the reaction between Al and NaCl, and increases, therefore, metal corrosion.

The addition of tin to aluminum has given, not only a positive effect on the activation of the aluminum, but also on its crystal structure which has become much more hard and resistant to mechanical shocks.

References

1. Reading JT, Newport JJ. Mater Protect. 1966; 5:15.
2. Perrault GG. J. Electrochem.Soc. 1979; 126:199.
3. Kabanov BN, Astakhovand II, Kiseleva JG. Electrochim Acta. 1979; 24:167.
4. Parsons R. Handbook of Electrochemical Constants. London: Butterworths;

- 1959.
5. Richardson JA, Wood GC. *Corrosion Sci.* 1970; 10: 313.
 6. Davis JA, Staklis AA, Watts AA. *Into Env Sci.* 17th Ann Tech Meet LA, 1971; 177.
 7. Brown BF, Fujii CT, Dahlberg EP. *J Electrochem Soc.* 1969;166: 218.
 8. Kitamura K, Sato E. *Keikin-zuku.* 1978; 29:563.
 9. Kurov OV, Melekov RL. *Zasch Metal.* 1979;15:314.
 10. Rosenfeld IL, Marshakov IK. *Corrosion.* 1964;20:115t.
 11. De Mecheli SM. *Corrosion Sci.* 1978;18:605.
 12. Edeleanu E, Evans UR. *Trans Faraday Soc.* 1951;47:1121.
 13. Marek M, Kinker JR, Hochman RF. 6th Int Congress Metallic Corrosion. Syneny; 1975.
 14. Gimenez P, Rameau JJ, Reboul MC. *Corrosion.* 1981;37:673.
 15. Dexter SC. *Corrosion.* 1980;36:423-432.
 16. Hilger JP, Boulahrouf A. *Mater Charact.* 1990;24:159.